

1 **Retinal horizontal cells use different synaptic sites for global**
2 **feedforward and local feedback signaling**

3

4 Christian Behrens¹⁻⁴, Yue Zhang^{1,2,4}, Shubhash Chandra Yadav⁵, Silke Haverkamp⁶, Stephan
5 Irsen⁷, Maria M. Korympidou^{1,2,4}, Anna Schaedler^{1,2,4}, Karin Dedek⁵, Robert G. Smith⁸,
6 Thomas Euler¹⁻³, Philipp Berens^{1-3,9}, Timm Schubert^{1,2}

7

8 ¹*Institute for Ophthalmic Research, University of Tübingen, 72076 Tübingen, Germany*

9 ²*Center for Integrative Neuroscience, University of Tübingen, 72076 Tübingen, Germany*

10 ³*Bernstein Center for Computational Neuroscience, University of Tübingen, 72076 Tübingen, Germany*

11 ⁴*Graduate Training Centre of Neuroscience, University of Tübingen, 72076 Tübingen, Germany*

12 ⁵*Neurosensorics/Animal Navigation, Institute for Biology and Environmental Sciences, University of Oldenburg,*
13 *26111 Oldenburg, Germany*

14 ⁶*Department of Computational Neuroethology, Center of Advanced European Studies and Research (caesar),*
15 *53175 Bonn, Germany*

16 ⁷*Department of Electron Microscopy and Analytics, Center of Advanced European Studies and Research*
17 *(caesar), 53175 Bonn, Germany*

18 ⁸*Department of Neuroscience, University of Pennsylvania, Philadelphia, PA 19104, USA*

19 ⁹*Institute for Bioinformatics and Medical Informatics, University of Tübingen, 72076 Tübingen, Germany*

20 **Abstract**

21 In the outer plexiform layer (OPL) of the mouse retina, two types of cone photoreceptors (cones)
22 provide input to more than a dozen types of cone bipolar cells (CBCs). This transmission is modulated
23 by a single horizontal cell (HC) type, the only interneuron in the outer retina. Horizontal cells form
24 feedback synapses with cones and feedforward synapses with CBCs. However, the exact
25 computational role of HCs is still debated. Along with performing global signaling within their
26 laterally coupled network, HCs also provide local, cone-specific feedback. Specifically, it has not been
27 clear which synaptic structures HCs use to provide local feedback to cones and global forward
28 signaling to CBCs.

29 Here, we reconstructed in a serial block-face electron microscopy volume the dendritic trees of
30 five HCs as well as cone axon terminals and CBC dendrites to quantitatively analyze their
31 connectivity. In addition to the fine HC dendritic tips invaginating cone axon terminals, we also
32 identified “bulbs”, short segments of increased dendritic diameter on the primary dendrites of HCs.
33 These bulbs are located well below the cone axon terminal base and make contact to other cells mostly
34 identified as other HCs or CBCs. Using immunolabeling we show that HC bulbs express vesicular
35 gamma-aminobutyric acid transporters and co-localize with GABA receptor $\gamma 2$ subunits. Together,
36 this suggests the existence of two synaptic strata in the mouse OPL, spatially separating cone-specific
37 feedback and feedforward signaling to CBCs. A biophysics-based computational model of a HC
38 dendritic branch supports the hypothesis that the spatial arrangement of synaptic contacts allows
39 simultaneous local feedback and global feedforward signaling.

40 **Introduction**

41 At the very first synapse of the mouse visual system, the signal from the cone photoreceptors (cones)
42 is relayed to second-order neurons: each cone axon terminal has more than 10 output sites, contacting
43 a sample of the 13 types of cone bipolar cells (CBCs) (Wässle et al. 2009; Tsukamoto and Omi 2014;
44 Behrens et al. 2016), which relay the signal ‘vertically’ to retinal output neurons, the retinal ganglion
45 cells. In a complementary circuit, laterally-organized horizontal cells (HCs) modulate the
46 photoreceptor-BC synapse (Haverkamp, Grünert, and Wässle 2000). Each ON-cone bipolar cell (ON-
47 CBC) dendrite invaginates the cone axon terminal to contact an individual cone output site and forms
48 a triad with HC dendritic processes, whose distal dendritic tips also invaginate the synaptic cleft,
49 flanking ON-CBC dendrites. In contrast, OFF-CBC dendrites contact the cone axon terminal base
50 without forming contacts with HC dendritic tips (reviewed in Diamond 2017) (Fig. 1a).

51 Horizontal cells are thought to play a major role in global visual processing and to contribute
52 to contrast enhancement and generation of center-surround receptive fields, providing global feedback
53 signals to cones and feedforward signals to BCs (reviewed in Thoreson and Mangel 2012;
54 Drinnenberg et al. 2018; Ströh et al. 2018). Functional measurements indicate that HCs provide local
55 feedback to photoreceptors (Jackman et al. 2011; Chapot et al. 2017), modulating each cone’s output
56 individually. However, the role of this local feedback is unclear in the context of the HC’s traditional
57 role of providing global feedback.

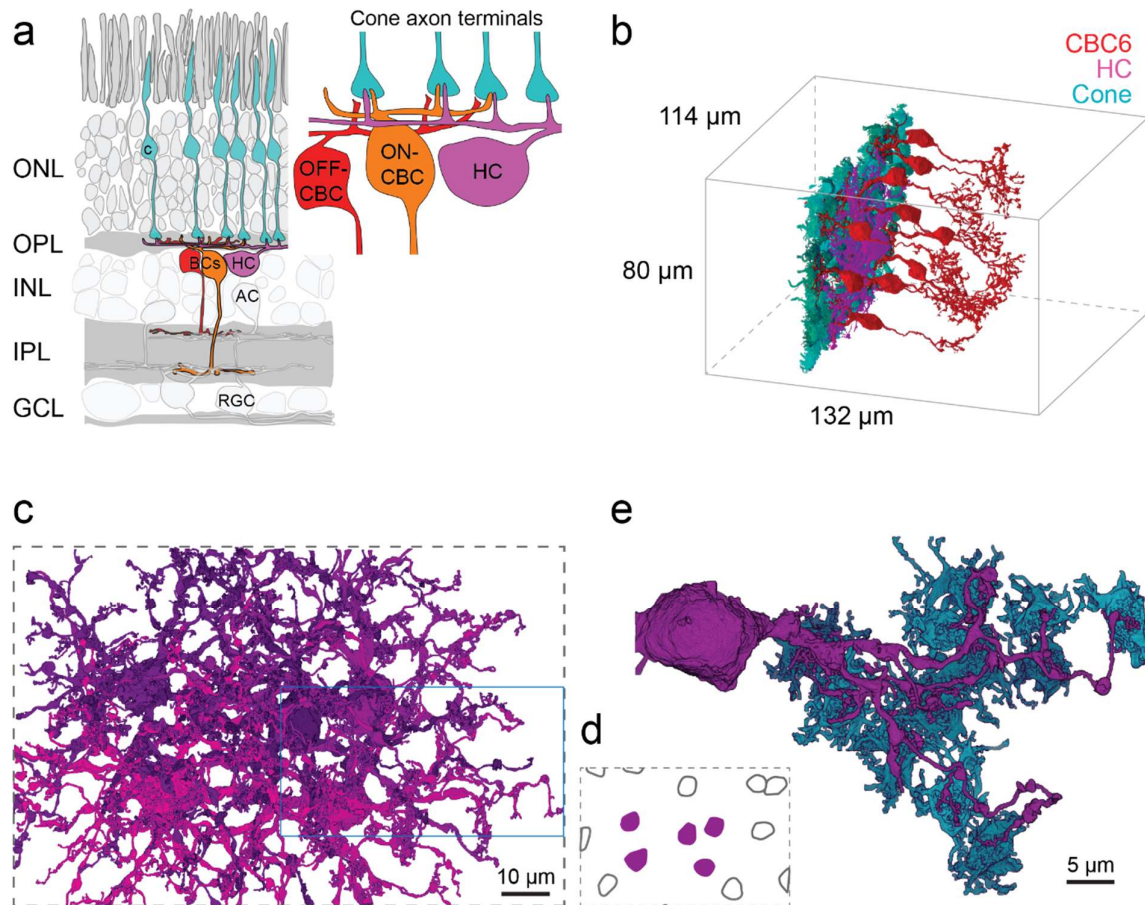
58 In addition, synapses between HCs and BCs were observed in in electron microscopic studies
59 over three decades ago but have not been further investigated (Olney 1968; Kolb 1977; Linberg and
60 Fisher 1988). Thus, despite our increasing knowledge of the complex interplay of different synaptic
61 mechanisms underlying HC feedback to cones (Liu et al. 2013; Kemmler et al. 2014; Vroman et al.
62 2014; Grove et al. 2019), a quantitative anatomical picture of the outer retinal connectivity with the
63 HC as a central player is missing.

64 Here, we made use of the serial block face electron microscopy dataset e2006 (Helmstaedter et al.
65 2013) to reconstruct the outer mouse retina with a focus on the HC circuitry and identify the
66 connectivity motifs made between HCs and other neuron types. In addition to the invaginating
67 contacts between cones and HCs in the cone axon terminal, we identified and quantitatively assessed –
68 at the level of primary HC dendrites – putative GABAergic synapses among HCs as well as between
69 HCs and CBCs as previously hypothesized (Dowling, Brown, and Major 1966; Marchiafava 1978;
70 Yang and Wu 1991; Duebel et al. 2006). Based on a biophysical model of HC signaling, we propose
71 that a role of this putative second synaptic site in HCs is to provide global signals in the form of
72 GABAergic input to postsynaptic CBCs, complementing the local feedback provided directly to cones.
73 This suggests that a single interneuron can simultaneously provide local reciprocal feedback and
74 global feedforward signals at distinct synaptic locations.

75 **Results**

76 **Reconstruction of horizontal cells and connectivity with cone photoreceptors**

77 Using the publicly available serial block-face electron microscopy dataset e2006 (Helmstaedter et al.,
78 2013, Fig. 1b), we reconstructed five complete dendritic arbors of HCs in the outer mouse retina (Fig.
79 1c,d). We analyzed the contacts of all three classes of neurons in the outer retina – cones, BCs and
80 HCs (Helmstaedter et al. 2013; Behrens et al. 2016) – to gain a complete picture of outer retinal
81 connectivity. The reconstructed HCs had a dendritic area of $4,600 \pm 400 \mu\text{m}^2$ (mean \pm SD) with 4 to 6
82 primary dendrites leaving the soma ($n = 5$ HCs) and extended fine dendritic tips towards cone axon
83 terminals (Fig. 1e). Next, we analyzed the HC connectivity within the cone axon terminals (Fig. 2a).
84 Each HC contacted on average 61 ± 5 (between 51 and 77) cones; these were all cones within its
85 dendritic field. Interestingly, we found that cones closer to the HC somata were contacted with
86 significantly more fine HC tips than distal ones (Fig. 2b,c; Generalized Additive Model with smooth
87 term for distance from soma and random effect of specific HC, $p < 2 \cdot 10^{-16}$ for smooth term, see
88 Methods for details). In addition, the contact area – the area of close apposition between cell
89 membranes, a proxy for the probability of synaptic contacts (Helmstaedter et al. 2013) – between an
90 individual HC and cones followed the number of invaginating contact sites along the HC dendrite and
91 significantly decreased towards the HC's periphery (Fig. 2d; Generalized Additive Model with smooth
92 term for distance from soma and random effect of specific HC, $p = 4.2 \cdot 10^{-7}$ for smooth term).
93 Together this suggests that HCs get most input from cones close to their soma.



94
95

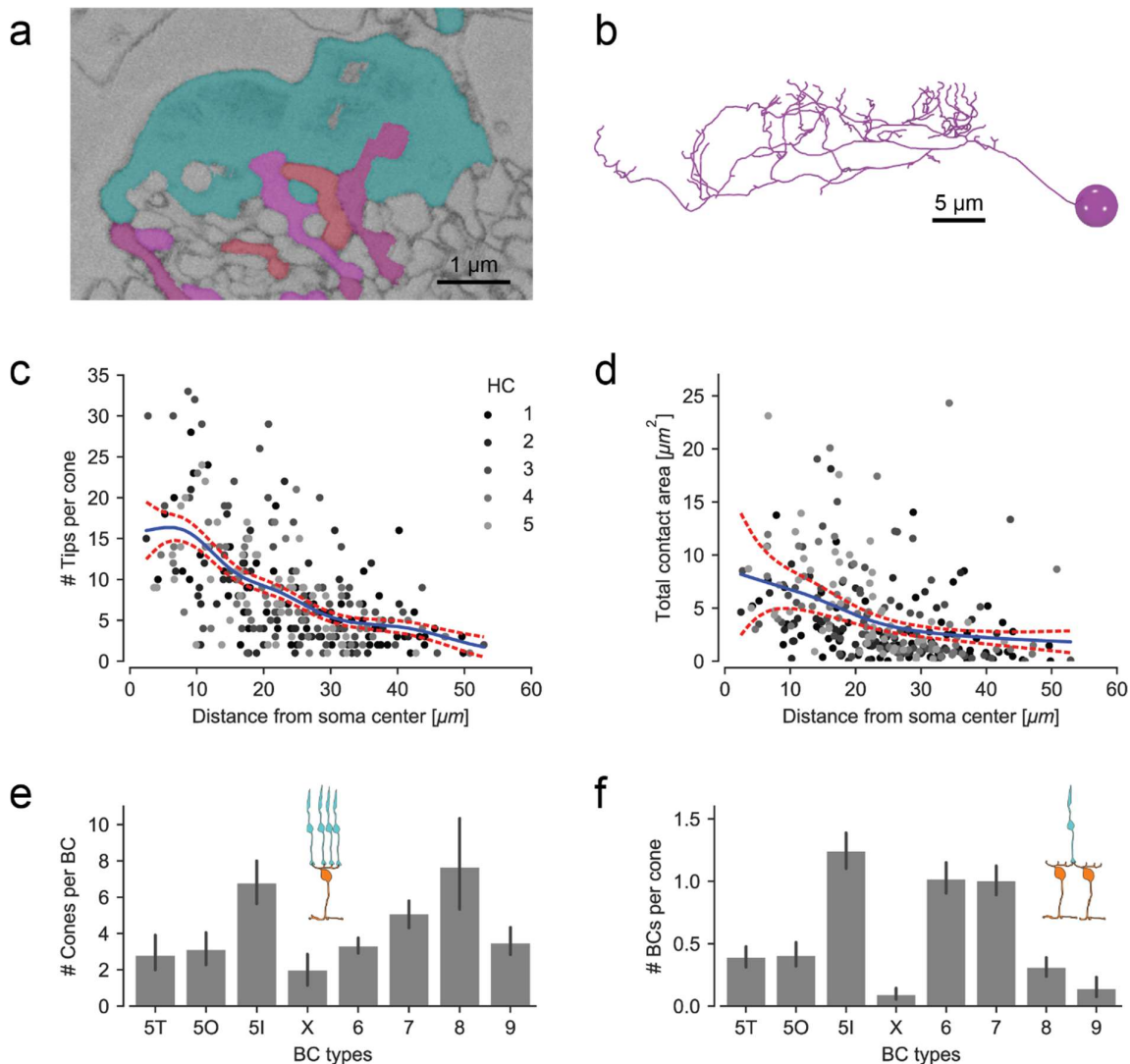
96 **Figure 1. Horizontal cell reconstruction.** (a) Schematic of a vertical section through the mouse
97 retina, highlighting the reconstructed cell types. Inset: Textbook-view of the connectivity of bipolar
98 cells (BCs) and horizontal cell (HCs) at the cone axon terminals with invaginating HC (magenta) and
99 ON-CBC (orange) dendritic tips and basal OFF-CBC contacts (red). AC, amacrine cell; RGC, retinal
100 ganglion cell. (b) Outlines of the dataset with volume reconstructed cone axon terminals (cyan), one
101 HC (magenta) and several CBC6 (red, 10 of 45 CBC6s shown). (c) Volume reconstructions of five
102 HCs (top view); blue rectangle: location of dendrite shown in (e). (d) Soma locations of the five
103 reconstructed HCs (magenta) and 10 HCs not reconstructed (black outline) HCs. (e) Bottom view of
104 the volume reconstruction of a complete HC dendrite (magenta) with contacted cone axon terminals
105 (cyan). HC dendrite taken from inset in (c).

106
107

108 **Invaginating contacts between cones, ON-cone bipolar cells and horizontal cells**

109 We found that the connectivity between cones and their postsynaptic partners was the typical "triad
110 synapse" motif, where HC tips in the synaptic cleft are closely associated with invaginating dendrites
111 of ON-CBCs. A previous study found that some ON-CBC types such as CBC types 5T, 5O, 8 and X
112 sampled sparsely from cones (Fig. 2e; see also Fig. 3 in Behrens et al. 2016). In addition, the CBCX
113 made rather small basal but not 'typical' invaginating contacts at the cone axon terminal, more
114 resembling OFF-CBC contacts. If these BC types contacted cones more sparsely, the number of
115 contacts with invaginating HC dendrites should be lower as well. We checked all ON-CBC contacts

116 (n = 36) at five central cones (making contacts with all 5 reconstructed HCs) and identified one or two
 117 invaginating HC dendritic tips per ON-CBC tip for all contacts. This typical "triad" motif implies that
 118 the number of contacts between HCs and ON-CBCs matches the number of cone contacts per CBC.
 119 Thus, the number of contacts between HCs and BC types CBC5T, 5O, 8 and X within the cone axon
 120 terminal is lower than for the other ON-CBC types (Fig. 2f).
 121



122
 123

124 **Figure 2. Horizontal cell-to-cone and HC-to-ON-CBC contacts** (a) EM slice showing a cone axon
 125 terminal (cyan) with invaginating contacts from an ON-CBC (red) and a HC (magenta). (b) Vertical
 126 view of the skeleton model of the HC branch from Fig. 1e illustrating the increase of the number of
 127 dendritic tips towards the soma. (c) HC skeleton tips per contacted cone vs. distance from HC soma.
 128 Blue: Poisson GAM fit with 95%-confidence interval (red). (d) Contact area between HC and cone
 129 axon terminal volume reconstructions per cone vs. distance from HC soma. Blue: Gamma GAM fit
 130 with 95%-confidence interval (red). (e) Contacted cones per BC for all CBC types. (f) BCs contacted
 131 per cone for all CBC types. Number of ON-BCs contacting each cone per type. Both (e) and (f)
 132 redrawn using data from Behrens et al. 2016. Error bars show 95% CI.

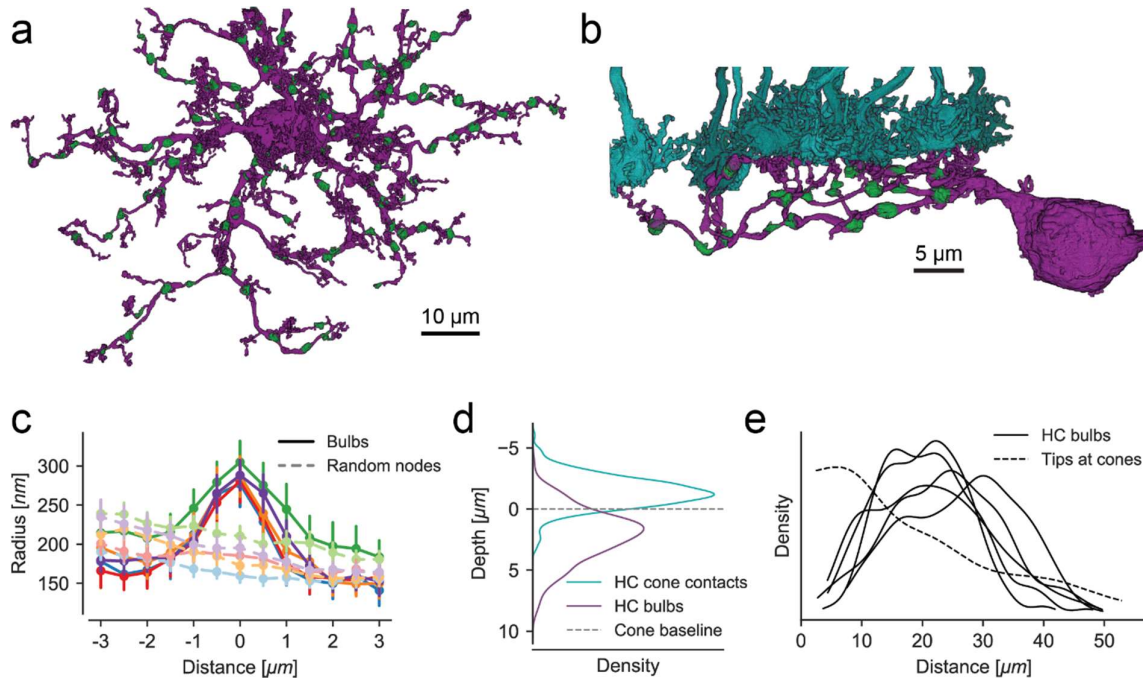
133 **Non-invaginating (bulb) contacts between horizontal cells and bipolar cells**

134 Horizontal cell feedback modulates the cones' glutamate release directly within the invaginating cleft
135 (Kamermans et al. 2001). For a spatially uniform stimulus pattern, this feedback should be spatially
136 correlated and should affect the output of all cones similarly. However, for a spatially uncorrelated
137 stimulus pattern, HC distal tips would receive uncorrelated input and provide uncorrelated feedback to
138 neighboring cones. Indeed, HC dendritic tips have been shown to feature highly localized signals
139 (Jackman et al. 2011; Chapot et al. 2017), making it possible to relay highly localized feedback to
140 individual cones. Yet, in addition to transmitting local uncorrelated signals, for spatially uniform
141 stimuli, this pathway may be also responsible for global signals traditionally suggested as a general
142 role of HCs (Thoreson and Mangel 2012; Drinnenberg et al. 2018). The reason is that, while the local
143 feedback from a HC distal tip to its presynaptic cone will attenuate the local signal received by the HC
144 distal tip, the global signal transmitted from HC dendrites and soma is not attenuated.

145 However, a second synaptic output pathway where HCs could provide direct GABAergic
146 output to BC dendrites independent from the invaginating cleft has been postulated (Marchiafava
147 1978; Yang and Wu 1991; Duebel et al. 2006). Because dendrites of OFF-CBCs have a low and
148 dendrites of ON-CBCs have a high chloride level (Duebel et al. 2006), GABA released by HCs that
149 binds to GABA-gated chloride membrane channels in CBC dendrites will hyperpolarize an OFF-CBC
150 and depolarize an ON-CBC. Therefore, an antagonistic surround in both ON- and OFF-CBCs can be
151 generated by HCs through this lateral feedforward pathway. This feedforward signaling pathway could
152 integrate both correlated and/or uncorrelated HCs signals along the HC primary dendrites generating a
153 global output signal which is then relayed to BCs. However, such a synaptic HC-BC connection has
154 not been identified so far.

155 In search of this synaptic site between HCs and CBCs, we systematically examined the five
156 volume-rendered HCs and found regularly distributed, dendritic swellings along the primary dendrites
157 (Fig. 3a,b). These dendritic swellings (bulbs) showed a marked increase in dendritic diameter (Fig.
158 3c). Almost all bulbs were located clearly below the cone axon terminal base and not in direct contact
159 with it (Fig. 3b,d). In contrast to invaginating dendritic tips that showed a higher density towards the
160 soma of the HC, the bulbs were more regularly distributed along the primary dendrites (Fig. 3e).

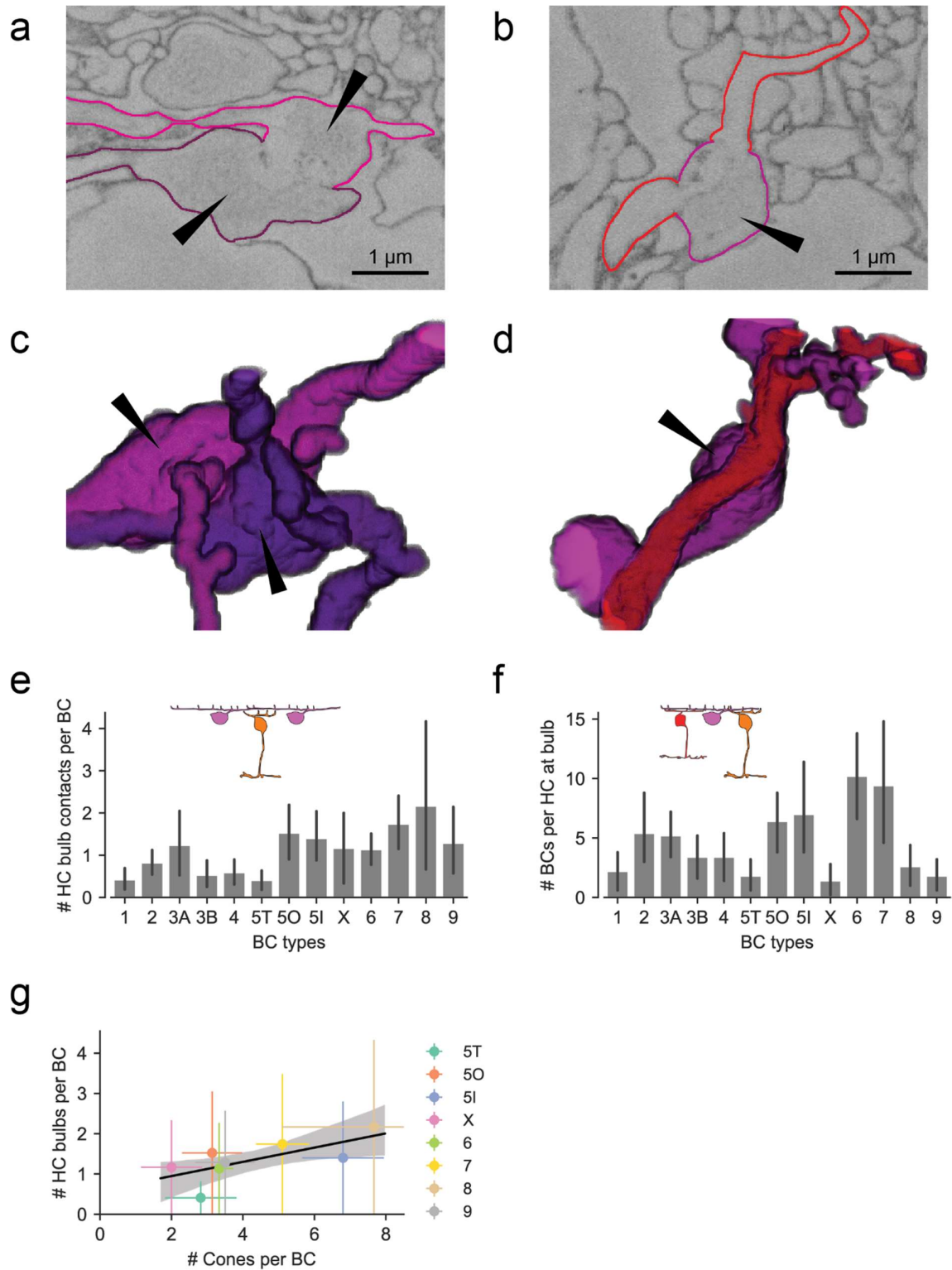
161 Most of the identified bulbs contacted either bulbs of other volume-rendered HCs (67 out of
162 545, Fig. 4a,c) or dendrites of ON- and OFF-CBCs (219 out of 545; Fig. 4b,d) or both (69), suggesting
163 that the bulb structures represent potential HC-HC and/or HC-BC synapses. For the remaining 190
164 bulbs, we had no information about the identity of the contacted cells. As only five HCs were traced,
165 these contacts may well represent contacts to other HCs and/or BCs that were not traced because their
166 soma was located outside the EM stack.



167

168

169 **Figure 3. Identification of bulbs in horizontal cells.** (a) Top view of a reconstructed HC with bulbs
170 highlighted in green. (b) Side view of a branch from the same HC with bulbs (green) and cone axon
171 terminals (cyan). (c) Dendritic radius profile at bulb locations (solid curves w/high saturation)
172 compared to randomized points on the dendrites (dashed curves w/low saturation) with matching
173 distribution of distances from soma and tips. (d) Depth of bulbs compared to HC-to-cone contacts. (e)
174 Kernel density estimate of the distance distribution of bulbs relative to the soma for all five HCs.
175 Dashed line: Model fit showing distribution of HC skeleton tips at cones from Fig. 2c.



176

177 **Figure 4. Horizontal cell bulb contacts with other neurons.** (a) EM slice showing bulb contact
 178 between two HCs. (b) Bulb contact between HC (magenta) and ON-CBC (red). (c) Volume-rendered
 179 contact site between bulbs from two HCs. (d) Volume-rendered contact site between HC (magenta)
 180 bulb (arrowhead) and ON-CBC dendrite (red). (e) HC bulb contacts per BC for all CBC types. (f) BCs
 181 contacted by bulbs per HC for all CBC types. (g) Bulb contacts vs. contacted cones for all ON-CBC
 182 types (data from (e) and Fig. 2e) with linear regression. All error bars show 95% CIs.

183 Interestingly, we found a difference in bulb-level connectivity between HCs and OFF-CBCs
184 vs. HCs and ON-CBCs: the majority of ON-CBCs contacted HCs at the bulb site (except for CBC5T);
185 all OFF-CBC types made considerably fewer contacts than ON-CBCs (except CBC3A) (Fig. 4e).
186 However, the overall number of contacts per CBC is likely underestimated since contacts to not
187 reconstructed HCs are not included (see above). Furthermore, the number of BCs contacted at bulbs
188 per HC was lowest for the CBC types 5T, X, 8 and 9 and highest for CBC types 6 and 7 (Fig. 4f). For
189 types X, 8 and 9, the low numbers likely originate in their lower cell count while for CBC5T (which
190 has the same dendritic density as CBC5O and 5I cells) it is a consequence of the low number of
191 contacts per CBC. Comparing the bulb-to-ON-CBC contacts with the number of cone-to-ON-CBC
192 contacts taken from our recent study (Behrens et al. 2016) showed that both connectivity patterns are
193 almost identical for nearly all BC types (Fig. 2e,4e). The only striking difference was found within the
194 group of CBC5 cells: CBC5T has the lowest contact number with both HC bulbs and cones whereas
195 CBC5I made many contacts with both cones and bulbs. CBC5O sampled from as few cones as
196 CBC5T but made more bulb contacts, similar to CBC5I (Fig. 4g). Thus, while the morphological
197 properties such as density, dendritic field size, axon terminal size and stratification depth of the three
198 ‘sister’ types of CBC5 do not differ much, they can be distinguished based on their connectivity
199 patterns with cones and HCs in the outer retina.

200

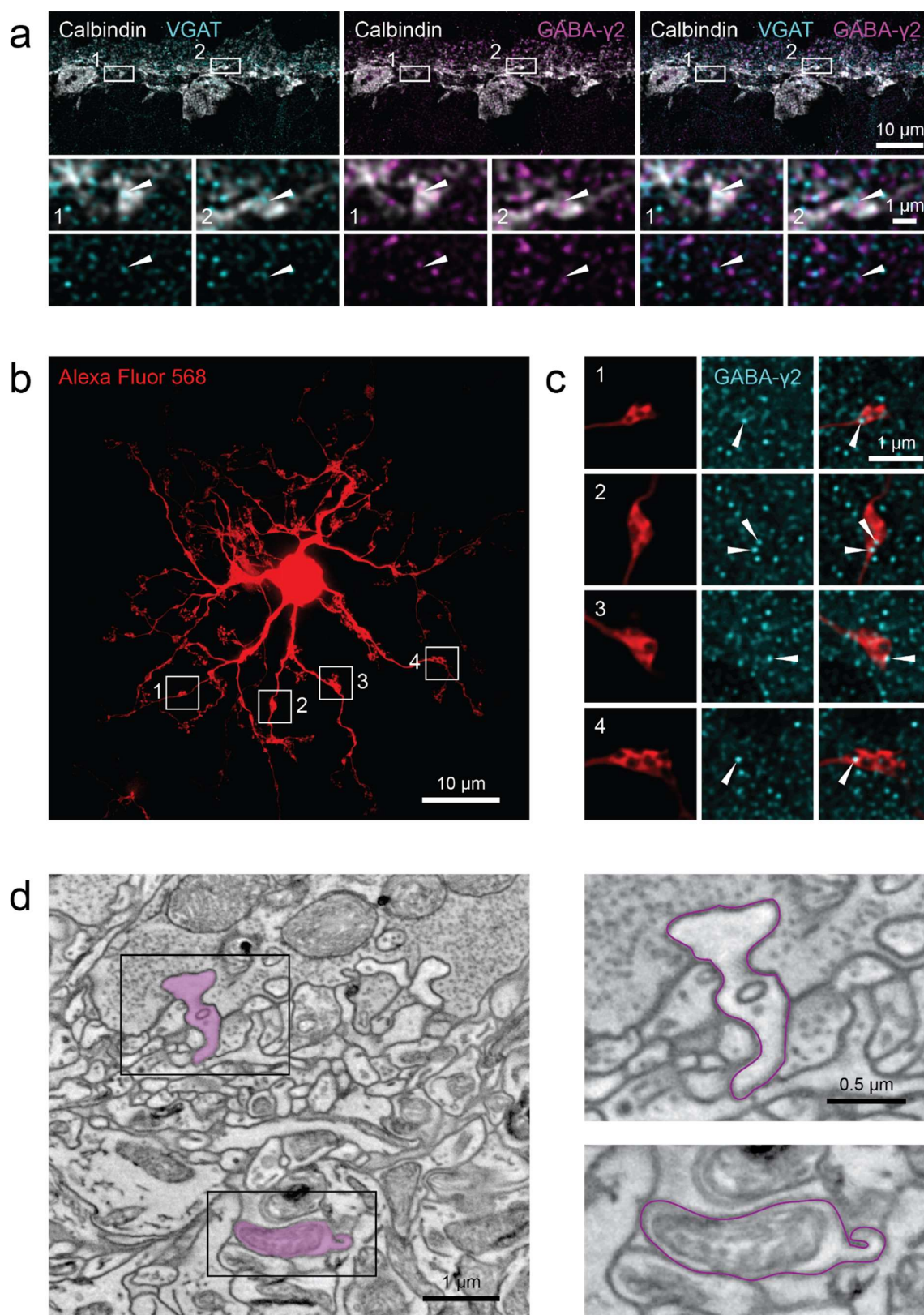
201 **Horizontal cell bulbs are putative synaptic structures**

202 If HC bulbs indeed formed presynaptic sites to relay global cone signals, one would expect
203 presynaptic proteins to be co-localized with these bulbs. In mammalian HCs, several presynaptic
204 proteins are associated with synaptic vesicles, including the vesicular gamma-aminobutyric acid
205 transporter (VGAT) (Guo et al. 2009; Cueva et al. 2002). However, most immunolabeling studies of
206 the OPL have focused on the distal tips of HCs rather than their primary dendrites. To identify
207 potential presynaptic sites along HC dendrites, we therefore used calbindin and VGAT antibodies to
208 visualize HCs and presynaptic vesicles, respectively (Fig. 5a). Indeed, we found intense VGAT
209 staining in dendritic thickenings at the same depth at which bulbs were found in the EM data.

210 If bulbs are the site of GABAergic synapses between HCs and to BCs, then GABA receptors
211 should be present at VGAT-positive bulbs as well. In the mouse retina, different GABA receptor
212 subunits are expressed in the outer retina: A ‘dashed’ band of a GABA receptor $\alpha 1$ subunit staining
213 can be seen at the level of the cone axon terminals (Haverkamp and Wässle 2000), indicating that $\alpha 1$
214 subunits are prominently expressed by HC dendritic tips invaginating in the synaptic cleft (Kemmler et
215 al. 2014). In contrast, GABA receptor $\gamma 2$ subunits have a broader expression profile that clearly
216 stratifies below the cone axon terminals (Haverkamp and Wässle 2000). Indeed, we found that VGAT
217 and GABA receptor $\gamma 2$ subunit immunolabeling co-localized on bulb-like structures (representative
218 example shown in Fig. 5a; similar results were obtained in four out of four immunostainings from two
219 different mice). To assess GABA receptor distribution on individual bulbs, we injected HCs in the

220 whole-mount preparation with the fluorescent dye Alexa Fluor 568 and then performed GABA
221 receptor immunolabeling (Fig. 5b,c). The $\gamma 2$ subunit immunoreactivity was strong at the level of the
222 primary dendrites and all identified bulbs (n = 30 bulbs in n = 3 injected HCs) showed
223 immunolabeling for the GABA receptor $\gamma 2$ subunit, indicating that bulbs may provide and/or receive
224 GABAergic input (Fig. 5c). Sources for GABAergic input may be other HCs (Liu et al. 2013) or
225 eventually interplexiform amacrine cells (Witkovsky, Gábel, and Križaj 2008; Dedek et al. 2009).

226 For further evidence that the GABA receptors in bulbs may be synaptic structures, we
227 performed focused ion beam scanning EM and reconstructed HCs from their dendritic tips in the
228 invaginating cleft (Fig. 5d, left) to the depth in the OPL where bulbs are located. In this EM image
229 stack, bulbs could be identified based on their thickened structure (Fig. 5d, supplementary image
230 stack). These structures always contained mitochondria which are typically found in presynaptic
231 structures (n = 7 bulbs) (Gala et al. 2017). However, compared with the glutamate-filled vesicles in the
232 cone axon terminal, the vesicles in both invaginating tips and bulbs of HCs were barely detectable
233 (Fig. 5d). Thus, the vesicle distribution was not further investigated (see Discussion).



235 **Figure 5. Synaptic structures at horizontal cell bulb contacts.** (a) Calbindin labeled HCs with
236 VGAT (cyan) and GABA receptor gamma2 (magenta) immunolabeling in vertical outer retinal
237 section. Arrowheads indicate co-localization on primary dendrites. (b) Alexa Fluor 568-injected HC
238 with identified bulbs (white boxes indicate examples). (c) Enlarged bulbs (red) from boxes in (b) with
239 GABA receptor $\gamma 2$ immunolabeling (cyan). Arrowheads indicate co-localization. (d) Electron
240 microscopy image showing a manually traced HC (magenta) with a dendritic tip invaginating in the
241 cone axon terminal (upper right) and the primary dendrite below the cone axon terminal with a HC
242 bulb of the same cell (lower right). Note the mitochondrial structure in the bulb. Black rectangles:
243 location of magnifications shown on the right.

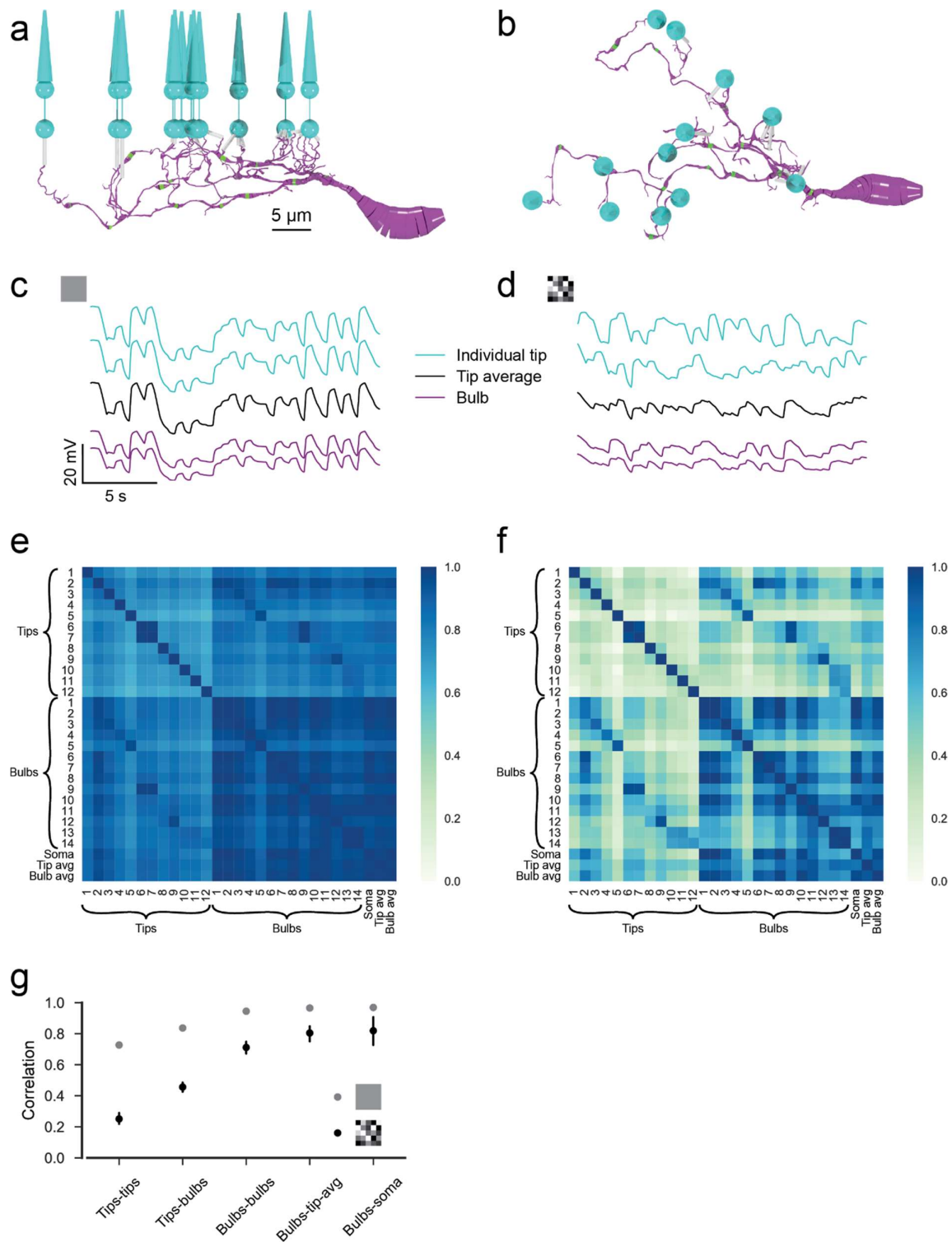
244

245

246 **Biophysical modelling indicates potential bulb function**

247 To study the potential functional role of HC bulb contacts, we built a biophysical model of a HC
248 dendritic branch with cone input (Fig. 6a,b) based on our previously published model (Chapot et al.
249 2017). We stimulated the cones in the model with either full-field or checkerboard noise for spatially
250 correlated and uncorrelated input, respectively, and measured voltage signals in the HC dendritic tips
251 invaginating into cone axon terminals ($n = 12$) and in the bulb structures ($n = 14$) (Fig. 6c,d). For full-
252 field stimuli, we found high correlations between voltage signals from all recording points ($0.85 \pm$
253 0.10). Due to vesicle release noise included in the model, which occurred independently at each
254 synapse between cones and HC tips, correlations between signals in different tips (0.73 ± 0.07) and
255 between signals in tips and bulbs (0.84 ± 0.06) were lower than those between signals in bulbs ($0.94 \pm$
256 0.04) (Fig. 6e). However, correlations between bulbs and the average over the tip signals (0.97 ± 0.02)
257 were similar to the correlations between bulbs.

258 For the checkerboard noise, which is a spatially maximally uncorrelated stimulus, the result
259 was different: The average correlation between voltage signals in tips was rather low (0.25 ± 0.14),
260 confirming our previous results (Chapot et al. 2017). In contrast, the average correlation between
261 voltage signals in bulbs was much higher (0.71 ± 0.19) and so was the correlation between bulb signal
262 and the average over the tip signals (0.80 ± 0.10) (Fig. 6g). Together, this indicates that for a natural
263 stimulus with spatially uncorrelated stimulation pattern, the global component of the stimulus
264 dominates the signal at the level of the bulbs whereas the local signal at the HC dendritic tips can be
265 used for feedback to individual cones (Fig. 7).



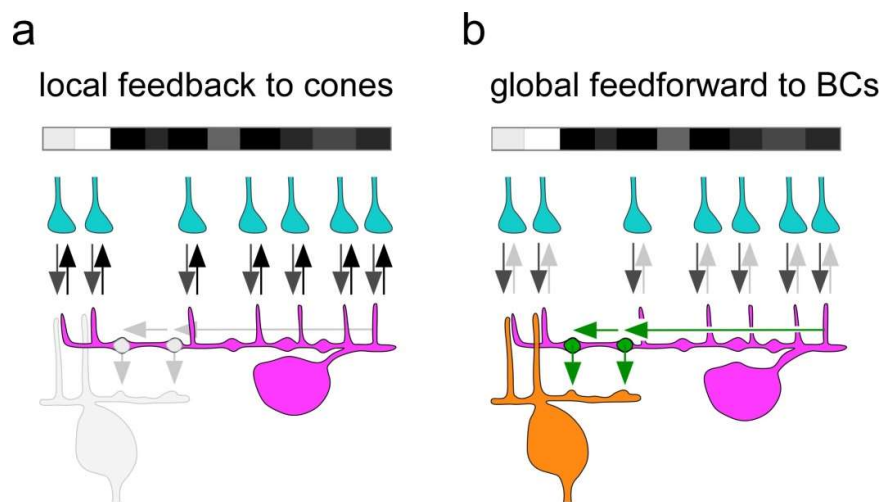
266

267 **Figure 6. Biophysical modelling.** (a) Side and (b) top view of the modelled HC dendrite with bulbs
 268 (green) and cones (cyan). (c) & (d) Example voltage traces recorded at HC dendritic tips below cones,
 269 at bulbs and average over all tips for (c) a random full-field noise stimulus and (d) a random
 270 checkerboard noise stimulus without synaptic vesicle release noise. (e) & (f) Correlations from 60 s of
 271 (e) full-field and (f) checkerboard stimulation including synaptic vesicle release noise. (g) Mean
 272 correlations between different tips, between tips and bulbs, between different bulbs, bulbs and the tip
 273 mean and bulbs and the soma for both stimuli. avg, average.

274 Discussion

275 Classically, HCs have been postulated to perform global computations like gain control and contrast
276 normalization (Barnes, Merchant, and Mahmud 1993; Verweij, Kamermans, and Spekreijse 1996;
277 Drinnenberg et al. 2018). However, local signaling in HCs has recently been reported in a number of
278 studies (Jackman et al. 2011; Chapot et al. 2017; Grove et al. 2019), raising the important question,
279 how a strongly electrically coupled syncytium of a laterally organized interneuron can perform both
280 local and global computations and relay them to its presynaptic partners. Here, we provide a
281 quantitative picture of connectivity in the outer retina including HCs and describe a new putative
282 synaptic site in HCs. In contrast to the well-described feedback synapse that modulates the cone
283 output, this putative synapse is likely a feedforward synapse that provides GABAergic drive to other
284 HCs as well as to BCs. On the functional level, it likely relays an integrated, global signal, resulting
285 from multiple local signals from numerous cones. This global output signal may contribute to the
286 global center-surround organization of bipolar cells, as has long been posited (Werblin and Dowling
287 1969; Schwartz 1974). (Fig. 7).

288
289



290

291 **Figure 7. Synaptic circuitry of horizontal cells in the outer mouse retina.** (a) Dendritic tips of a
292 HC (magenta) receive cone input (grey arrows) and provide local and cone-specific feedback (black
293 arrows) to cone axon terminals (cyan) in the presence of a spatially and temporally uncorrelated white
294 noise stimulus (white/grey/black bar). (b) For the same uncorrelated stimulus, the cone input signals
295 (grey arrows) are integrated to a global signal in the HC dendrite (green arrow) and forwarded by a
296 BC-contacting bulb (green) to the BC (orange) forming the surround signal.

297 **Horizontal cell bulbs are likely synaptic structures**

298 Based on few ultrastructural electron microscopic examples of chemical synapses between HCs and
299 BCs shown in earlier years (Olney 1968; Kolb 1977; Linberg and Fisher 1988), these direct synaptic
300 connections have long been suggested (Miller and Dacheux 1976; Marchiafava 1978; Yang and Wu
301 1991; Vardi et al. 2000; Duebel et al. 2006). However, these connections have never been
302 systematically investigated. Here, we used the e2006 EM data set that was initially used to describe
303 inner retinal connections (Helmstaedter et al. 2013) and photoreceptor-to-BC synapses (Behrens et al.
304 2016). The majority (~65%) of identified HC bulbs was contacted by other HC bulbs and/or BC
305 dendrites indicating that bulbs were not randomly distributed dendritic thickenings. This finding was
306 supported by the uniform distribution of bulbs across the HC dendritic tree suggesting the overall
307 mosaic organization of the mouse retina is maintained at this synaptic level. Furthermore, we found
308 that the bulbs contained mitochondria required to supply energy for the presynaptic vesicle release
309 mechanism as described for a reciprocal amacrine cell synapse in the cat retina (Ellias and Stevens
310 1980). Indeed, we found synaptic proteins on HC bulbs such as VGAT and GABA γ 2 receptors on HC
311 bulbs that represent pre- and postsynaptic markers, respectively. However, which retinal cell type(s)
312 express the GABA receptors is still unclear. Since the bulbs contact other HC bulbs as well as BC
313 dendrites, it is conceivable that the bulbs represent a general GABAergic output site to postsynaptic
314 cells (reviewed in Diamond 2017).

315 Unfortunately, we could not detect any neurotransmitter vesicles at HC bulbs in our EM
316 images – a problem that was reported for HCs decades ago (Dowling and Boycott 1966) and may be
317 attributed to methodological limitations of the dataset. However, in an earlier cat retina study, vesicle
318 clusters in HC dendrites were found to be “...typically organized around some denser particles...”
319 (Fig. 18 in Kolb 1977). In addition, in the mouse retina, “...the synaptic complex, was of conventional
320 configuration, involved the horizontal cell presynaptically, and was always found in the innermost
321 aspect of the outer plexiform layer...” (Fig. 11 in Olney 1968) – this is where we found the majority of
322 bulbs in our study. Another reason why we did not find vesicles could be the (somewhat unlikely)
323 GABA secretion by GABA transporters as shown in the fish retina (Schwartz 1987). Additionally, we
324 also cannot exclude the possibility that bulbs receive direct glutamatergic input by diffusion from
325 photoreceptors – similar to OFF-CBCs – however, the distance of HC bulbs from the release sites in
326 cones axon terminals appears to be relatively large compared with the OFF-CBC dendrites that
327 directly contact the axon terminal. Hence, we propose that GABA release at the bulbs results from
328 electrical signal propagation along the dendrites of the HCs rather than being initiated via diffusing
329 glutamate.

330 A GABAergic synapse between HCs along with a depolarizing chloride level in HCs (Miller
331 and Dacheux 1976; Kamermans and Werblin 1992) could transmit a lateral signal between them,
332 similar to the lateral signal spread within the syncytium formed by electrical synapses. One might
333 therefore imagine that mouse HC bulbs could represent sites of gap junctions - electrical synapses

334 between HCs (He, Weiler, and Vaney 2000). However, the vast majority of connexin57 protein
335 forming electrical synapses in mouse HCs is expressed at more distal sites on the HC dendrites and is
336 not very prominent on the bulb-bearing primary dendrites (Janssen-Bienhold et al. 2009). Thus, it is
337 unlikely that the role of HC bulbs is to couple HCs by electrical synapses.

338 Our finding of an additional synapse in the outer mouse retina may explain how HCs may
339 perform both feedback to cones and feedforward signaling to BCs simultaneously, which may
340 contribute to understanding a longstanding enigma.

341

342 **Selective connectivity with ON-CBC types as a mechanism of synaptic scaling?**

343 As previously reported, we found some ON-CBCs contact cone axon terminals in a very specific
344 manner. For example, the CBC types 5T, 5O, X, 8 and 9 contact considerably fewer cones than
345 expected from their relatively large dendritic field whereas other types such as types 5I, 6 and 7
346 contact almost every cone located within their dendritic field (Behrens et al. 2016). Remarkably, this
347 connectivity is also reflected in the number of bulbs connected by ON-CBCs: Types 5T, X and 9
348 contact fewer bulbs than the other types while type 8 contacts only slightly more bulbs than other cells
349 despite its significantly larger dendritic field. This correlation of excitatory and inhibitory synapse
350 number may be a form of synaptic scaling (Turrigiano 2011) that could have an effect on the
351 functional organization of the receptive field of BCs. The center of a receptive field is defined as the
352 region that is driven by excitatory (i.e., direct glutamatergic) input from cones whereas the surround is
353 formed by the lateral inhibition by interneurons in the periphery. A balanced synaptic weight between
354 center and surround activation is likely to be crucial for the BC's ability to stay within the operational
355 range of its output synapses.

356 The only exception is the BC type 5O; it contacts only a few cones but has relatively many
357 bulb contacts, in strong contrast to the types 5T or 5I, which make few or many contacts to both cones
358 and HC bulbs, respectively. Based on their morphology and their stratification depth in the inner
359 plexiform layer, these three BC types are hardly distinguishable. However, they differ in their
360 connectivity with cones and HC bulbs in the outer retina, and thus, may be functionally distinct
361 regarding their receptive field properties (Franke et al. 2017). Whether the size and efficiency of
362 synaptic contacts is different and whether or how synaptic scaling is implemented for ON-CBC and
363 HC contacts has to be addressed in a future functional study.

364

365 **Functional consequences of a second synaptic layer in the outer retina**

366 For decades, an open question has remained about how lateral inhibition essential for center-surround
367 organization in the outer retina can be generated by fine structures such as the HC dendritic tips
368 invaginating into the cone axon terminal (Yang and Wu 1991). With the new putative synaptic site
369 described here between HCs and BCs, we propose a potential solution for this long existing dilemma
370 of how HCs provide global/local feedback to cones and global feedforward signaling to BCs. In our

371 view, HCs are a retinal interneuron with two functional specializations: feedback to cones and
372 feedforward synapses to BCs and other HCs.

373 A recent study showed that, based on their thin diameter and high resistance, the fine HC
374 dendritic tips are optimized for generation of local cone-specific feedback and to a lesser extent for
375 lateral propagation of electrical signals (Chapot et al. 2017). However, the extent to which the
376 feedback to cones is global or local strongly depends on the presented visual stimulus. For small-scale
377 non-correlated visual stimuli, the feedback is expected to be cone-specific and can differ significantly
378 for neighboring cones, strongly following the cone output signal. For a highly correlated visual
379 stimulus, the feedback would be similar at all dendritic tip synapses, thus generating a rather uniform,
380 global feedback pattern generated by correlated local activity.

381 The second synapse type made by HCs, the GABAergic bulb synapse, may be optimized for
382 the relay of global signals to other HCs and BCs that are modulated in at least three different ways:
383 First, all the photoreceptor input that reaches the primary HC dendrites and the bulb synapses would
384 be filtered by the feedback at the dendritic tip feedback synapses. Second, the spread along HC
385 dendrites is subject to passive filtering. Third, depending on the coupling state of the HC network, via
386 electrical synapses or depolarizing GABAergic synapses, signals in HC dendrites may be strengthened
387 or weakened. In any case, the global signal would be relayed to postsynaptic cells and contribute to
388 center-surround antagonistic receptive field organization.

389

390 **Interaction between global and local signaling pathways**

391 Under conditions with a rather uniform stimulation pattern, the local feedback from HCs to
392 photoreceptors is thought to include global (lateral) signals (Warren et al. 2016) because of the high
393 degree of correlation in the stimulus. Thus, HC feedback can accomplish both very local and spatially
394 extended (i.e., global) feedback control of synaptic release. With the uniform stimulation pattern used
395 in our model, the feedback to cones is correlated and is expected to be weak (Smith 1995). The reason
396 is that the local dendritic tip signal in HCs itself is attenuated by the local feedback and hardly
397 propagates over long distances along primary dendrites into other HC fine dendritic tips. Feedback is
398 necessary to regulate the synaptic release of cones to maintain the optimal operating point in the
399 output synapse, and thus to preserve the S/N ratio (Borghuis, Ratliff, and Smith 2018). However,
400 strong feedback can become unstable for high feedback loop gains and typical synaptic delays (Smith
401 1995). To prevent instability, the HC feedback includes an ephaptic mechanism which is fast with
402 minimal delay (Vroman et al. 2014; Chapot et al. 2017). However, the feedback strength is also
403 limited by the need to maintain high gain at the cone output to CBCs. In contrast, ‘simple’
404 feedforward inhibition is always stable and can use high signaling amplitudes. These functional
405 requirements constrain the feedback and feedforward synapses to be at structurally different synaptic
406 sites. In addition, the synaptic mechanisms – ephaptic/pH-mediated feedback and GABAergic
407 feedforward signaling – may contribute to the very specialized function of the two synapses: Whereas

408 the feedback synapse can decrease but also increase the cone output signal depending on the stimulus
409 context (Smith 1995; Kemmler et al. 2014), the bulb synapse only provides GABAergic drive. Its
410 feedforward signal to CBCs has a different role, of providing inhibition to balance the excitation in
411 CBCs, along with a stronger spatial surround than can be provided by the cone signal. Yet, both
412 feedback and feedforward HC signals will contribute to the surround in CBCs and all downstream
413 neurons.

414

415 **The horizontal cell – an interneuron with multiple functions**

416 Interneurons show a remarkable heterogeneity and diversity in both function and morphology in all
417 parts of the brain (reviewed in Cardin 2018). The morphology of an interneuron is thought to reflect its
418 function: In the retina, for instance, BCs relay signals from the outer to the inner synaptic layer,
419 whereas wide-field amacrine cells relay information laterally across the retina (reviewed in Euler et al.
420 2014; Diamond 2017). However, morphology can be deceiving; for example, the very symmetric
421 starburst amacrine cells in the mammalian retina compute the direction of image motion (Taylor and
422 Smith 2012). Moreover, some interneurons have been shown to serve more than one functional role
423 but do so in a context-dependent manner. For example, in low light conditions, AII amacrine cells are
424 central to the primary rod vision pathway, while under photopic conditions they change their role and
425 contribute to approach sensitivity (Münch et al. 2009). For A17 amacrine cells (Hartveit 1999) which
426 make reciprocal synapses with rod BCs a functional switch between local and more global processing
427 has been suggested (Schubert and Euler 2010). More intriguing is our finding that different synaptic
428 functions such as feedforward and feedback signaling of HCs are apparently performed
429 simultaneously at different synaptic sites as previously shown for the VG3 amacrine cell type in the
430 mouse retina that provides excitatory and inhibitory drive at distinct synaptic sites (Lee et al. 2016;
431 Tien, Kim, and Kerschensteiner 2016).

432 An interesting question is why local and global signaling – two different synaptic tasks – are
433 performed in the same interneuron in the mouse outer retina. Circuits of the inner retina seem rather to
434 be built from several types of neurons, each contributing a specific function. Maybe with few
435 exceptions – as illustrated by A17 and VG3 amacrine cells discussed above – amacrine cells, which
436 with ~45 types are the most diverse retinal interneuron, are thought to represent specific computational
437 tasks. Why is this motif not implemented in the outer retina? Two possible explanations may play a
438 role here: First, the cone axon terminal system is among the most complex synaptic structures in the
439 brain (Haverkamp, Grünert, and Wässle 2000). Therefore, integrating a second, dedicated interneuron
440 type during evolution may have been avoided for the sake of space limitation and circuitry
441 simplification. This hypothesis is supported by the fact that the reciprocal feedback synapses to rod
442 photoreceptors are not provided by an additional interneuron type but by an additional intraretinal
443 axon terminal system of HCs which is a unique structure for interneurons in the brain. Second, the
444 cones require a global feedback signal that represents the average background, so their synaptic vesicle

445 release can optimally represent a contrast signal (Srinivasan, Laughlin, and Dubs 1982). The most
446 straightforward mechanism to generate such a global feedback signal is through summation of many
447 local signals from individual cones. Although global feedback might be arranged at a separate synapse
448 from local feedback, it is most straightforward to provide this integrated signal as local/global
449 feedback to each cone to control its release rate.

450 **Methods**

451 **Dataset**

452 Our analysis is based on the SBEM dataset e2006 (Helmstaedter et al. 2013,
453 <https://www.neuro.mpg.de/connectomics>). The dataset covers a piece of mouse retina of 80 x 114 x
454 132 μm with a resolution of 25 x 16.5 x 16.5 nm. We identified the somata of 15 HCs and
455 skeletonized the dendrites of the five central HC in KNOSSOS (Helmstaedter, Briggman, and Denk
456 2011, www.knossostool.org). We used algorithms published with the dataset to reconstruct the
457 volumes of HCs, BCs and cone axon terminals in the OPL and to identify their contacts (for details see
458 Behrens et al. 2016).

459 We manually identified HC bulbs and their contacts. To compare the dendritic diameter
460 profile around the bulbs with the one of random points on the dendrite (Fig. 3c), we used the Vaa3D-
461 Neuron2 auto-tracing (Xiao and Peng 2013) to get a simplified representation of the HC morphologies
462 from the volume reconstruction, consisting of a regularly spaced grid of nodes with associated
463 diameters. For each bulb position we identified the closest node and extracted the dendritic diameter
464 profile around it. For a fair comparison to average points on the dendrite, we draw a random set of
465 nodes with distributions of average distances from soma and tips matching the bulb locations.

466 To calculate the statistics of HC-to-BC contacts at bulbs, we included only BCs where the center of
467 the BC dendritic field was within the dendritic field of at least one of the reconstructed HC. With this
468 method, the numbers in Fig. 4e,f are a lower bound. For the HCs, additional contacts on branches
469 ending outside the dataset are possible as well as contacts from BCs with soma outside of the dataset,
470 especially for larger types such as CBC8 and CBC9. The number of bulb contacts per CBC is
471 underestimated as well since the true coverage factor of HC dendrites lies at about 5-7 while we have
472 only five overlapping HCs in the center and coverage going down to one towards the edges of the
473 dataset.

474

475 **Horizontal cell injections and immunolabeling for GABA receptors**

476 Three HCs were injected using Alexa Fluor 568 as described before (Yadav, Tetenborg, and Dedek
477 2019). In brief, cell nuclei in the retinal whole-mount preparation were visualized with DAPI labeling.
478 Based on depth and size of the nuclei, HCs were identified and then injected with Alexa Fluor 568
479 using sharp electrodes and subsequently fixed using 4% paraformaldehyde. Retinal whole-mounts
480 were then incubated in primary antibodies, and immunolabeling for the GABA receptor subunit $\gamma 2$
481 was carried as previously described (Ströh et al. 2013). Immunolabeling for VGAT and the GABA
482 receptor subunit $\gamma 2$ was carried out using fixed 12 μm thick vertical retina sections using standard
483 protocols with primary antibodies against VGAT, the $\gamma 2$ subunit and calbindin and secondary
484 antibodies. All images were taken with a Leica TCS SP8 confocal microscope. Data was deconvolved
485 with Huygens Essential software, using a theoretical point spread function and further processed using
486 Fiji (Schindelin et al. 2012).

487 **Three-Dimensional Electron Microscopy using FIB-SEM**

488 Focused ion beam-scanning electron microscopy (FIB-SEM tomography) allows efficient, complete,
489 and automatic 3D reconstruction of HC dendrites with a resolution comparable to that of TEM (Xu et
490 al. 2017; Bosch et al. 2015). An adult mouse (male, 14 weeks) was deeply anesthetized with isoflurane
491 and decapitated before the eyes were dissected. All procedures were approved by the local animal care
492 committee and were in accordance with the law for animal experiments issued by the German
493 government (Tierschutzgesetz). The posterior eyecups were immersion fixed in a solution containing
494 0.1 M cacodylate buffer, 4% sucrose and 2% glutaraldehyde, and then rinsed in 0.15 M cacodylate
495 buffer. A 1×1 mm² retina piece was stained in a solution containing 1% osmium tetroxide, 1.5%
496 potassium ferrocyanide, and 0.15 M cacodylate buffer. The osmium stain was amplified with 1%
497 thiocarbohydrazide and 2% osmium tetroxide. The retina was then stained with 2% aqueous uranyl
498 acetate and lead aspartate. The tissue was dehydrated through an 70-100% ethanol series, transferred
499 to propylene oxide, infiltrated with 50%/50% propylene oxide/Epon Hard, and then 100% Epon Hard.
500 The Epon Hard block was hardened at 60°C.

501 Afterwards, the block was prepared for FIB-SEM tomography. The sample was trimmed using
502 an ultramicrotome (Leica UC 7) and afterwards glued onto a special sample stub (caesar workshop)
503 using conductive silver paint. To avoid charge artifacts, all surfaces of the block were sputter-coated
504 with 30 nm AuPd (80/20). A focused ion dual beam (FIB) workstation (XB 1540, Carl Zeiss
505 Microscopy, Oberkochen, Germany) was used for tomogram acquisition. This instrument uses a
506 focused gallium ion beam that can mill the sample at an angle of 54° with respect to the electron beam.
507 A digital 24-bit scan-generator (ATLAS5, Carl Zeiss) was used to control ion and electron beam. The
508 sample was milled using an ion beam of 1nA at an energy of 30 kV. Images were collected at an
509 energy of 2 kV using a pixel size of 5 x 5 nm (x,y) and a layer thickness of 15 nm (z). Milling and
510 imaging was performed simultaneously to compensate for charging effects. The raw images were
511 converted into an image stack, black areas were cropped, and the images were aligned using cross
512 correlation (Mastrorade 1997). HC dendrites were manually identified in ImageJ.

513

514 **Modelling**

515 We built a biophysically realistic model of a HC dendritic branch using the simulation language
516 NeuronC (Smith 1992). We used Vaa3D-Neuron2 auto-tracing (Xiao and Peng 2013) to generate a
517 .swc file from the volume reconstruction of one HC branch and manually refined it in Neuromantic
518 (Myatt et al. 2012). The model contains voltage-gated Ca²⁺ and K⁺ channels with different channel
519 densities for proximal and distal dendrites and AMPA-type glutamate receptors at the cone synapses
520 (Tab. 1). Photoreceptors were modelled as predefined in NeuronC with two compartments including
521 voltage-gated Ca²⁺ and Ca²⁺-activated Cl⁻ channels. Cones were placed at the original positions with
522 one synapse per invaginating HC dendritic tip found in the EM data. The synapses to the HC include
523 postsynaptic AMPA channels modelled as Markov state-machines that included vesicle release noise.

524 The model was stimulated for 60 s with both full-field and checkerboard Gaussian noise with a
525 temporal frequency of 2 Hz and equal variance. The checkerboard stimulus consisted of independent
526 pixels of 5 x 5 μm size such that all cones were stimulated independently. Voltage signals were
527 recorded in a dendritic tip below each of the 12 cones and in 14 bulbs identified along the dendrite.

528

529 **Statistics**

530 Error bars in all plots are 95% confidence intervals (CIs) calculated as percentiles of the bootstrap
531 distribution obtained via case resampling. In Figure 2c,d, we fitted generalized additive models (R
532 package mgcv, Wood 2017) with Poisson output distribution for skeleton tips (Fig. 2c) and Gamma
533 output distribution for contact area (Fig. 2d). Both had distance from soma as a smooth function and
534 HC identity as smooth random effect.

535

536

537 **Acknowledgments**

538 We thank Helmstaedter et al. 2013 for making their data available and L. Peichl for critical reading of
539 the manuscript. This work was supported by the German Research Foundation (DFG) through
540 individual grants (SCHU2243/3-1 to TS, BE5601/2-1 to PB) and the priority program SPP2041
541 (BE5601/4-1 to PB, EU 42/9-1 to TE), the German Ministry of Education and Research through the
542 Bernstein Award (FKZ 01GQ1601 to PB) and NIH grants (EY023766 to TE & RGS; EY022070 to
543 RGS).

544 **Tables**

545

Rm	[Ω cm ²]		2,500
Ri	[Ω cm]		200
Channel densities			
L-type Ca ²⁺ channels	[S/cm ²]	Soma and proximal dendrites	3e-4
		Distal dendrites	1e-3
K ⁺ channels	[S/cm ²]	Soma and proximal dendrites	1e-5
		Distal dendrites	1e-5

546

547 **Table 1. Parameters of the biophysical model.**

548 **References**

- 549 Barnes, S., Merchant, V., & Mahmud, F. 1993. “Modulation of Transmission Gain by Protons at the
550 Photoreceptor Output Synapse.” *Proceedings of the National Academy of Sciences* 90 (21):
551 10081–85. <https://doi.org/10.1073/pnas.90.21.10081>.
- 552 Behrens, C., Schubert, T., Haverkamp, S., Euler, T., & Berens, P. 2016. “Connectivity Map of Bipolar
553 Cells and Photoreceptors in the Mouse Retina.” *ELife* 5 (November): 065722.
554 <https://doi.org/10.7554/eLife.20041>.
- 555 Borghuis, B.G., Ratliff, C.P., & Smith, R.G. 2018. “Impact of Light-Adaptive Mechanisms on
556 Mammalian Retinal Visual Encoding at High Light Levels.” *Journal of Neurophysiology* 119
557 (4): 1437–49. <https://doi.org/10.1152/jn.00682.2017>.
- 558 Bosch, C., Martí-nez, A., Masachs, N., Teixeira, C.M., Fernaud, I., Ulloa, F., Pérez-Martí-nez, E., et
559 al. 2015. “FIB/SEM Technology and High-Throughput 3D Reconstruction of Dendritic Spines
560 and Synapses in GFP-Labeled Adult-Generated Neurons.” *Frontiers in Neuroanatomy* 9 (May).
561 <https://doi.org/10.3389/fnana.2015.00060>.
- 562 Cardin, J.A. 2018. “Inhibitory Interneurons Regulate Temporal Precision and Correlations in Cortical
563 Circuits.” *Trends in Neurosciences* 41 (10): 689–700. <https://doi.org/10.1016/j.tins.2018.07.015>.
- 564 Chapot, C.A., Behrens, C., Rogerson, L.E., Baden, T., Pop, S., Berens, P., Euler, T., & Schubert, T.
565 2017. “Local Signals in Mouse Horizontal Cell Dendrites.” *Current Biology* 27 (23): 3603-
566 3615.e5. <https://doi.org/10.1016/j.cub.2017.10.050>.
- 567 Cueva, J.G., Haverkamp, S., Reimer, R.J., Edwards, R., Wässle, H., & Brecha, N.C. 2002. “Vesicular
568 γ -Aminobutyric Acid Transporter Expression in Amacrine and Horizontal Cells.” *Journal of*
569 *Comparative Neurology* 445 (3): 227–37. <https://doi.org/10.1002/cne.10166>.
- 570 Dedek, K., Breuninger, T., Sevilla Müller, L.P. de, Maxeiner, S., Schultz, K., Janssen-Bienhold, U.,
571 Willecke, K., Euler, T., & Weiler, R. 2009. “A Novel Type of Interplexiform Amacrine Cell in
572 the Mouse Retina.” *European Journal of Neuroscience* 30 (2): 217–28.
573 <https://doi.org/10.1111/j.1460-9568.2009.06808.x>.
- 574 Diamond, J.S. 2017. “Inhibitory Interneurons in the Retina: Types, Circuitry, and Function.” *Annual*
575 *Review of Vision Science* 3 (1): 1–24. <https://doi.org/10.1146/annurev-vision-102016-061345>.
- 576 Dowling, J.E., & Boycott, B.B. 1966. “Organization of the Primate Retina: Electron Microscopy.”
577 *Proceedings of the Royal Society B: Biological Sciences* 166 (1002): 80–111.
578 <https://doi.org/10.1098/rspb.1966.0086>.

- 579 Dowling, J.E., Brown, J.E., & Major, D. 1966. "Synapses of Horizontal Cells in Rabbit and Cat
580 Retinas." *Science* 153 (3744): 1639–41. <https://doi.org/10.1126/science.153.3744.1639>.
- 581 Drinnenberg, A., Franke, F., Morikawa, R.K., Jüttner, J., Hillier, D., Hantz, P., Hierlemann, A.,
582 Azeredo da Silveira, R., & Roska, B. 2018. "How Diverse Retinal Functions Arise from
583 Feedback at the First Visual Synapse." *Neuron* 99 (1): 117-134.e11.
584 <https://doi.org/10.1016/j.neuron.2018.06.001>.
- 585 Duebel, J., Haverkamp, S., Schleich, W., Feng, G., Augustine, G.J., Kuner, T., & Euler, T. 2006.
586 "Two-Photon Imaging Reveals Somatodendritic Chloride Gradient in Retinal ON-Type Bipolar
587 Cells Expressing the Biosensor Clomeleon." *Neuron* 49 (1): 81–94.
588 <https://doi.org/10.1016/j.neuron.2005.10.035>.
- 589 Ellias, S.A., & Stevens, J.K. 1980. "The Dendritic Varicosity: A Mechanism for Electrically Isolating
590 the Dendrites of Cat Retinal Amacrine Cells?" *Brain Research* 196 (2): 365–72.
591 [https://doi.org/10.1016/0006-8993\(80\)90401-1](https://doi.org/10.1016/0006-8993(80)90401-1).
- 592 Euler, T., Haverkamp, S., Schubert, T., & Baden, T. 2014. "Retinal Bipolar Cells: Elementary
593 Building Blocks of Vision." *Nature Reviews Neuroscience* 15 (8): 507–19.
594 <https://doi.org/10.1038/nrn3783>.
- 595 Franke, K., Berens, P., Schubert, T., Bethge, M., Euler, T., & Baden, T. 2017. "Inhibition Decorrelates
596 Visual Feature Representations in the Inner Retina." *Nature* 542 (7642): 439–44.
597 <https://doi.org/10.1038/nature21394>.
- 598 Gala, R., Lebrecht, D., Sahlender, D.A., Jorstad, A., Knott, G., Holtmaat, A., & Stepanyants, A. 2017.
599 "Computer Assisted Detection of Axonal Bouton Structural Plasticity in in Vivo Time-Lapse
600 Images." *ELife* 6: 1–20. <https://doi.org/10.7554/elife.29315>.
- 601 Grove, J.C.R., Hirano, A.A., los Santos, J. de, McHugh, C.F., Purohit, S., Field, G.D., Brecha, N.C., &
602 Barnes, S. 2019. "Novel Hybrid Action of GABA Mediates Inhibitory Feedback in the
603 Mammalian Retina." *PLOS Biology* 17 (4): e3000200.
604 <https://doi.org/10.1371/journal.pbio.3000200>.
- 605 Guo, C., Stella, S.L., Hirano, A.A., & Brecha, N.C. 2009. "Plasmalemmal and Vesicular γ -
606 Aminobutyric Acid Transporter Expression in the Developing Mouse Retina." *The Journal of*
607 *Comparative Neurology* 512 (1): 6–26. <https://doi.org/10.1002/cne.21846>.
- 608 Hartveit, E. 1999. "Reciprocal Synaptic Interactions Between Rod Bipolar Cells and Amacrine Cells
609 in the Rat Retina." *Journal of Neurophysiology* 81 (6): 2923–36.
610 <https://doi.org/10.1152/jn.1999.81.6.2923>.

- 611 Haverkamp, S., Grünert, U., & Wässle, H. 2000. “The Cone Pedicle, a Complex Synapse in the
612 Retina.” *Neuron* 27 (1): 85–95. [https://doi.org/10.1016/S0896-6273\(00\)00011-8](https://doi.org/10.1016/S0896-6273(00)00011-8).
- 613 Haverkamp, S., & Wässle, H. 2000. “Immunocytochemical Analysis of the Mouse Retina.” *The
614 Journal of Comparative Neurology* 424 (1): 1–23. [https://doi.org/10.1002/1096-
615 9861\(20000814\)424:1<1::AID-CNE1>3.0.CO;2-V](https://doi.org/10.1002/1096-9861(20000814)424:1<1::AID-CNE1>3.0.CO;2-V).
- 616 He, S., Weiler, R., & Vaney, D.I. 2000. “Endogenous Dopaminergic Regulation of Horizontal Cell
617 Coupling in the Mammalian Retina.” *Journal of Comparative Neurology* 418 (1): 33–40.
618 [https://doi.org/10.1002/\(SICI\)1096-9861\(20000228\)418:1<33::AID-CNE3>3.0.CO;2-J](https://doi.org/10.1002/(SICI)1096-9861(20000228)418:1<33::AID-CNE3>3.0.CO;2-J).
- 619 Helmstaedter, M., Briggman, K.L., & Denk, W. 2011. “High-Accuracy Neurite Reconstruction for
620 High-Throughput Neuroanatomy.” *Nature Neuroscience* 14 (8): 1081–88.
621 <https://doi.org/10.1038/nn.2868>.
- 622 Helmstaedter, M., Briggman, K.L., Turaga, S.C., Jain, V., Seung, H.S., & Denk, W. 2013.
623 “Connectomic Reconstruction of the Inner Plexiform Layer in the Mouse Retina.” *Nature* 500
624 (7461): 168–74. <https://doi.org/10.1038/nature12346>.
- 625 Jackman, S.L., Babai, N., Chambers, J.J., Thoreson, W.B., & Kramer, R.H. 2011. “A Positive
626 Feedback Synapse from Retinal Horizontal Cells to Cone Photoreceptors.” *PLoS Biology* 9 (5).
627 <https://doi.org/10.1371/journal.pbio.1001057>.
- 628 Janssen-Bienhold, U., Trümpner, J., Hilgen, G., Schultz, K., Sevilla Muller, L.P. De, Sonntag, S.,
629 Dedek, K., Dirks, P., Willecke, K., & Weiler, R. 2009. “Connexin57 Is Expressed in Dendro-
630 Dendritic and Axo-Axonal Gap Junctions of Mouse Horizontal Cells and Its Distribution Is
631 Modulated by Light.” *Journal of Comparative Neurology* 513 (4): 363–74.
632 <https://doi.org/10.1002/cne.21965>.
- 633 Kamermans, M., Fahrenfort, I., Schultz, K., Janssen-Bienhold, U., Sjoerdsma, T., & Weiler, R. 2001.
634 “Hemichannel-Mediated Inhibition in the Outer Retina.” *Science* 292 (5519): 1178–80.
635 <https://doi.org/10.1126/science.1060101>.
- 636 Kamermans, M., & Werblin, F.S. 1992. “GABA-Mediated Positive Autofeedback Loop Controls
637 Horizontal Cell Kinetics in Tiger Salamander Retina.” *The Journal of Neuroscience* 12 (7):
638 2451–63. <https://doi.org/10.1523/JNEUROSCI.12-07-02451.1992>.
- 639 Kemmler, R., Schultz, K., Dedek, K., Euler, T., & Schubert, T. 2014. “Differential Regulation of Cone
640 Calcium Signals by Different Horizontal Cell Feedback Mechanisms in the Mouse Retina.”
641 *Journal of Neuroscience* 34 (35): 11826–43. <https://doi.org/10.1523/JNEUROSCI.0272-14.2014>.
- 642 Kolb, H. 1977. “The Organization of the Outer Plexiform Layer in the Retina of the Cat: Electron

- 643 Microscopic Observations.” *Journal of Neurocytology* 6 (2): 131–53.
644 <https://doi.org/10.1007/BF01261502>.
- 645 Lee, S., Zhang, Y., Chen, M., & Zhou, Z.J. 2016. “Segregated Glycine-Glutamate Co-Transmission
646 from VGlut3 Amacrine Cells to Contrast-Suppressed and Contrast-Enhanced Retinal Circuits.”
647 *Neuron* 90 (1): 27–34. <https://doi.org/10.1016/j.neuron.2016.02.023>.
- 648 Linberg, K.A., & Fisher, S.K. 1988. “Ultrastructural Evidence That Horizontal Cell Axon Terminals
649 Are Presynaptic in the Human Retina.” *The Journal of Comparative Neurology* 268 (2): 281–97.
650 <https://doi.org/10.1002/cne.902680211>.
- 651 Liu, X., Hirano, A.A., Sun, X., Brecha, N.C., & Barnes, S. 2013. “Calcium Channels in Rat Horizontal
652 Cells Regulate Feedback Inhibition of Photoreceptors through an Unconventional GABA- and
653 PH-Sensitive Mechanism.” *The Journal of Physiology* 591 (13): 3309–24.
654 <https://doi.org/10.1113/jphysiol.2012.248179>.
- 655 Marchiafava, P.L. 1978. “Horizontal Cells Influence Membrane Potential of Bipolar Cells in the
656 Retina of the Turtle.” *Nature* 275 (5676): 141–42. <https://doi.org/10.1038/275141a0>.
- 657 Mastronarde, D.N. 1997. “Dual-Axis Tomography: An Approach with Alignment Methods That
658 Preserve Resolution.” *Journal of Structural Biology* 120 (3): 343–52.
659 <https://doi.org/10.1006/jsbi.1997.3919>.
- 660 Miller, R.F., & Dacheux, R.F. 1976. “Synaptic Organization and Ionic Basis of on and off Channels in
661 Mudpuppy Retina. I. Intracellular Analysis of Chloride-Sensitive Electrogenic Properties of
662 Receptors, Horizontal Cells, Bipolar Cells, and Amacrine Cells.” *The Journal of General
663 Physiology* 67 (6): 639–59. <https://doi.org/10.1085/jgp.67.6.639>.
- 664 Münch, T.A., Silveira, R.A. Da, Siebert, S., Viney, T.J., Awatramani, G.B., & Roska, B. 2009.
665 “Approach Sensitivity in the Retina Processed by a Multifunctional Neural Circuit.” *Nature
666 Neuroscience* 12 (10): 1308–16. <https://doi.org/10.1038/nn.2389>.
- 667 Myatt, D.R., Hadlington, T., Ascoli, G.A., & Nasuto, S.J. 2012. “Neuromantic – from Semi-Manual to
668 Semi-Automatic Reconstruction of Neuron Morphology.” *Frontiers in Neuroinformatics* 6
669 (March): 1–14. <https://doi.org/10.3389/fninf.2012.00004>.
- 670 Olney, J.W. 1968. “An Electron Microscopic Study of Synapse Formation, Receptor Outer Segment
671 Development, and Other Aspects of Developing Mouse Retina.” *Investigative Ophthalmology &
672 Visual Science* 7 (3): 250–68. <http://www.ncbi.nlm.nih.gov/pubmed/5655873>.
- 673 Schindelin, J., Arganda-Carreras, I., Frise, E., Kaynig, V., Longair, M., Pietzsch, T., Preibisch, S., et
674 al. 2012. “Fiji: An Open-Source Platform for Biological-Image Analysis.” *Nature Methods* 9 (7):

- 675 676–82. <https://doi.org/10.1038/nmeth.2019>.
- 676 Schubert, T., & Euler, T. 2010. “Retinal Processing: Global Players Like It Local.” *Current Biology*
677 20 (11): R486–88. <https://doi.org/10.1016/j.cub.2010.04.034>.
- 678 Schwartz, E.A. 1974. “Responses of Bipolar Cells in the Retina of the Turtle.” *The Journal of*
679 *Physiology* 236 (1): 211–24. <https://doi.org/10.1113/jphysiol.1974.sp010431>.
- 680 ———. 1987. “Depolarization without Calcium Can Release Gamma-Aminobutyric Acid from a
681 Retinal Neuron.” *Science* 238 (4825): 350–55. <https://doi.org/10.1126/science.2443977>.
- 682 Smith, R.G. 1992. “NeuronC: A Computational Language for Investigating Functional Architecture of
683 Neural Circuits.” *Journal of Neuroscience Methods* 43 (2–3): 83–108.
684 [https://doi.org/10.1016/0165-0270\(92\)90019-A](https://doi.org/10.1016/0165-0270(92)90019-A).
- 685 ———. 1995. “Simulation of an Anatomically Defined Local Circuit: The Cone-Horizontal Cell
686 Network in Cat Retina.” *Visual Neuroscience* 12 (03): 545–61.
687 <https://doi.org/10.1017/S0952523800008440>.
- 688 Srinivasan, M. V, Laughlin, S.B., & Dubs, A. 1982. “Predictive Coding: A Fresh View of Inhibition in
689 the Retina.” *Proceedings of the Royal Society of London. Series B. Biological Sciences* 216
690 (1205): 427–59. <https://doi.org/10.1098/rspb.1982.0085>.
- 691 Ströh, S., Puller, C., Swirski, S., Hölzel, M.-B., Linde, L.I.S. van der, Segelken, J., Schultz, K., et al.
692 2018. “Eliminating Glutamatergic Input onto Horizontal Cells Changes the Dynamic Range and
693 Receptive Field Organization of Mouse Retinal Ganglion Cells.” *The Journal of Neuroscience* 38
694 (8): 0141–17. <https://doi.org/10.1523/JNEUROSCI.0141-17.2018>.
- 695 Ströh, S., Sonntag, S., Janssen-Bienhold, U., Schultz, K., Cimiotti, K., Weiler, R., Willecke, K., &
696 Dedek, K. 2013. “Cell-Specific Cre Recombinase Expression Allows Selective Ablation of
697 Glutamate Receptors from Mouse Horizontal Cells.” *PLoS ONE* 8 (12): 15–17.
698 <https://doi.org/10.1371/journal.pone.0083076>.
- 699 Taylor, W.R., & Smith, R.G. 2012. “The Role of Starburst Amacrine Cells in Visual Signal
700 Processing.” *Visual Neuroscience* 29 (01): 73–81. <https://doi.org/10.1017/S0952523811000393>.
- 701 Thoreson, W.B., & Mangel, S.C. 2012. “Lateral Interactions in the Outer Retina.” *Progress in Retinal*
702 *and Eye Research* 31 (5): 407–41. <https://doi.org/10.1016/j.preteyeres.2012.04.003>.
- 703 Tien, N.W., Kim, T., & Kerschensteiner, D. 2016. “Target-Specific Glycinergic Transmission from
704 VGLUT3-Expressing Amacrine Cells Shapes Suppressive Contrast Responses in the Retina.” *Cell*
705 *Reports* 15 (7): 1369–75. <https://doi.org/10.1016/j.celrep.2016.04.025>.

- 706 Tsukamoto, Y., & Omi, N. 2014. “Some OFF Bipolar Cell Types Make Contact with Both Rods and
707 Cones in Macaque and Mouse Retinas.” *Frontiers in Neuroanatomy* 8 (September): 105.
708 <https://doi.org/10.3389/fnana.2014.00105>.
- 709 Turrigiano, G.G. 2011. “Stabilizing Neuronal Function Homeostatic Synaptic Plasticity: Local and
710 Global Mechanisms for Homeostatic Synaptic Plasticity: Local and Global Mechanisms for
711 Stabilizing Neuronal Function.” *Cold Spring Harb Perspect Biol*, 1–18.
712 <https://doi.org/10.1101/cshperspect.a005736>.
- 713 Vardi, N., Zhang, L.-L., Payne, J.A., & Sterling, P. 2000. “Evidence That Different Cation Chloride
714 Cotransporters in Retinal Neurons Allow Opposite Responses to GABA.” *The Journal of*
715 *Neuroscience* 20 (20): 7657–63. <https://doi.org/10.1523/JNEUROSCI.20-20-07657.2000>.
- 716 Verweij, J., Kamermans, M., & Spekreijse, H. 1996. “Horizontal Cells Feed Back to Cones by
717 Shifting the Cone Calcium-Current Activation Range.” *Vision Research* 36 (24): 3943–53.
718 [https://doi.org/10.1016/S0042-6989\(96\)00142-3](https://doi.org/10.1016/S0042-6989(96)00142-3).
- 719 Vroman, R., Klaassen, L.J., Howlett, M.H.C., Cenedese, V., Klooster, J., Sjoerdsma, T., &
720 Kamermans, M. 2014. “Extracellular ATP Hydrolysis Inhibits Synaptic Transmission by
721 Increasing PH Buffering in the Synaptic Cleft.” *PLoS Biology* 12 (5).
722 <https://doi.org/10.1371/journal.pbio.1001864>.
- 723 Warren, T.J., Hook, M.J. Van, Supuran, C.T., & Thoreson, W.B. 2016. “Sources of Protons and a Role
724 for Bicarbonate in Inhibitory Feedback from Horizontal Cells to Cones in *Ambystoma Tigrinum*
725 Retina.” *Journal of Physiology* 594 (22): 6661–77. <https://doi.org/10.1113/JP272533>.
- 726 Wässle, H., Puller, C., Müller, F., & Haverkamp, S. 2009. “Cone Contacts, Mosaics, and Territories of
727 Bipolar Cells in the Mouse Retina.” *The Journal of Neuroscience : The Official Journal of the*
728 *Society for Neuroscience* 29 (1): 106–17. <https://doi.org/10.1523/JNEUROSCI.4442-08.2009>.
- 729 Werblin, F.S., & Dowling, J.E. 1969. “Organization of the Retina of the Mudpuppy, *Necturus*
730 *Maculosus*. II. Intracellular Recording.” *Journal of Neurophysiology* 32 (3): 339–55.
731 <https://doi.org/10.1152/jn.1969.32.3.339>.
- 732 Witkovsky, P., Gábel, R., & Križaj, D. 2008. “Anatomical and Neurochemical Characterization of
733 Dopaminergic Interplexiform Processes in Mouse and Rat Retinas.” *The Journal of Comparative*
734 *Neurology* 510 (2): 158–74. <https://doi.org/10.1002/cne.21784>.
- 735 Wood, S.N. 2017. *Generalized Additive Models: An Introduction with R, Second Edition*. 2nd ed.
736 Chapman and Hall/CRC.
- 737 Xiao, H., & Peng, H. 2013. “APP2: Automatic Tracing of 3D Neuron Morphology Based on

- 738 Hierarchical Pruning of a Gray-Weighted Image Distance-Tree.” *Bioinformatics* 29 (11): 1448–
739 54. <https://doi.org/10.1093/bioinformatics/btt170>.
- 740 Xu, C.S., Hayworth, K.J., Lu, Z., Grob, P., Hassan, A.M., García-Cerdán, J.G., Niyogi, K.K., Nogales,
741 E., Weinberg, R.J., & Hess, H.F. 2017. “Enhanced FIB-SEM Systems for Large-Volume 3D
742 Imaging.” *ELife* 6: 1–36. <https://doi.org/10.7554/eLife.25916>.
- 743 Yadav, S.C., Tetenborg, S., & Dedek, K. 2019. “Corrigendum: Gap Junctions in A8 Amacrine Cells
744 Are Made of Connexin36 but Are Differently Regulated Than Gap Junctions in All Amacrine
745 Cells.” *Frontiers in Molecular Neuroscience* 12 (June): 1–2.
746 <https://doi.org/10.3389/fnmol.2019.00149>.
- 747 Yang, X., & Wu, S. 1991. “Feedforward Lateral Inhibition in Retinal Bipolar Cells: Input-Output
748 Relation of the Horizontal Cell-Depolarizing Bipolar Cell Synapse.” *Pnas* 88 (8): 3310–13.
749 <https://doi.org/10.1073/pnas.88.8.3310>.